

# A model of semimetallic behavior in strongly correlated electron systems

Stefan Blawid

*Max-Planck-Institut für Physik komplexer Systeme, Nöthnitzer Str. 38, 01187 Dresden, Germany*  
(October 8, 2018)

Metals with values of the resistivity and the Hall coefficient much larger than typical ones, e.g., of sodium, are called semimetals. We suggest a model for semimetals which takes into account the strong Coulomb repulsion of the charge carriers, especially important in transition-metal and rare-earth compounds. For that purpose we extend the Hubbard model by coupling one additional orbital per site via hybridization to the Hubbard orbitals. We calculate the spectral function, resistivity and Hall coefficient of the model using dynamical mean-field theory. Starting from the Mott-insulating state, we find a transition to a metal with increasing hybridization strength (“self-doping”). In the metallic regime near the transition line to the insulator the model shows semimetallic behavior. We compare the calculated temperature dependence of the resistivity and the Hall coefficient with the one found experimentally for  $\text{Yb}_4\text{As}_3$ . The comparison demonstrates that the anomalies in the transport properties of  $\text{Yb}_4\text{As}_3$  possibly can be assigned to Coulomb interaction effects of the charge carriers not captured by standard band structure calculations.

72.80.-r,71.10.-w,71.10.Fd,71.30.+h

## I. INTRODUCTION

Conventional semimetals like the pentavalent elements As, Sb and Bi can be well understood using the approximation of independent electrons. Having an even number of electrons per primitive cell, these solids indeed come very close to being insulators. They are not, because the occupied band nearest to the Fermi energy overlaps slightly with the unoccupied band lowest in energy. Therefore a few holes and a few electrons in these two bands can contribute to transport leading to a very small number of charge carriers  $n$ , as seen in the measured Hall coefficient  $R_H = 1/nec$  of these materials. However, the independent electron picture is often not appropriate to describe transition-metal and rare-earth compounds. Prominent examples are the transition-metal oxides like  $\text{V}_2\text{O}_3$ ,  $\text{MnO}$  or  $\text{NiO}$ . These oxides are insulators although they contain partially filled  $d$  bands. Already in 1949, Mott identifies the Coulomb interaction of the conduction electrons as reason for the insulating behavior<sup>1</sup>. Meanwhile, the term Mott insulator has become a synonym for solids with localized charge carriers due to their mutual Coulomb repulsion. In the early transition-metal oxides the movement of the charge carriers is completely blocked due to their mutual Coulomb repulsion. It seems likely that there also exist compounds in which the movement of the charge carriers is only nearly blocked and which exhibit therefore not insulating but semimetallic behavior. The aforementioned conventional semimetals As, Sb and Bi are solids which come close to being band insulators. There might exist transition-metal or rare-earth compounds which are semimetallic because they come close to being a Mott insulator. In Sec. IV we will discuss a possible example, the semimetal  $\text{Yb}_4\text{As}_3$ .

In this paper we want to investigate a simple model which is able to mimic a semimetal coming close to be-

ing a Mott insulator. Therefore we are heading for a model which can describe the transition from a Mott insulator to a metal by varying some control parameter. The appealing idea is that a metal near a quantum transition to an insulator behaves like a semimetal. This is so, because the conductivity vanishes for an insulator. Therefore resistivity and Hall coefficient should become very large if one approach the insulating state from the metallic side. It is important to note, that a non vanishing Hall coefficient can be only obtained in a non particle-hole-symmetric model. This excludes one possible candidate, the well-known Hubbard model with one electron per site. Here the control parameter would be the ratio between the kinetic and the Coulomb energy of the electrons which can be changed by applying pressure. A suited model system for our purpose is the self-doped Hubbard model introduced in Ref. 2. Here additional orbitals are coupled to a half-filled Hubbard model via hybridization. The additional electron states serve as a generic reservoir of charge. The hybridization drives the desired insulator-to-metal transition.

The self-doped Hubbard model is not based on purely academic considerations. It is inspired by the experimental observation of charge order in some transition-metal and rare-earth compounds like  $\text{Yb}_4\text{As}_3$  and  $\text{NaV}_2\text{O}_5$ . At high temperatures these compounds are mixed-valent systems. In  $\text{Yb}_4\text{As}_3$  for example the Yb-ions fluctuate between a twofold and threefold positive charged state leading to a formal valency of  $\text{Yb}^{2.25+}$ . At low temperatures the charges avoid their mutual Coulomb repulsion and stay as far apart as possible. In  $\text{Yb}_4\text{As}_3$  this leads to a static charge ordered state in which the nearest-neighbor sites of an  $\text{Yb}^{3+}$ -ion are only occupied by  $\text{Yb}^{2+}$ -ions and not by other  $\text{Yb}^{3+}$ -ions<sup>3-8</sup>. Therefore, the  $\text{Yb}^{3+}$ -ions are confined on a subsystem of all possible sites, here chains in  $\langle 111 \rangle$ -direction. A charge lattice is

superposed on the crystal lattice. In  $\text{Yb}_4\text{As}_3$  the charge order leads to a structural phase transition at  $T_c \approx 295\text{K}$ . The foremost equivalent Yb-sites split up in  $\text{Yb}^{2+}$ -sites with a crystal environment of lower symmetry and  $\text{Yb}^{3+}$ -site with one of higher symmetry. The superposed charge lattice manifest itself in the distorted crystal structure below 295K. It is important to note, that charge ordering drive a compound towards a Mott-insulating state because the confinement of the charges to a sublattice reduces their kinetic energy. Transition-metal or rare-earth compounds with a charge order transition are therefore promising candidates of systems coming close to being a Mott insulator. Indeed,  $\text{Yb}_4\text{As}_3$  is a semimetal<sup>9</sup>. A very simplified model have to contain sites preferential occupied by the charges representing the sublattice superposed by charge order. The charges are able to leave this sites to gain some kinetic energy. Therefore, the sites lower in energy have to be coupled to an empty reservoir of charges representing all other accessible but predominantly unoccupied sites of the crystal. The self-doped Hubbard model is a possible realization of this idea. To take advantage of sophisticated many-body techniques, namely the dynamical mean-field theory<sup>10,11</sup>, the empty reservoir of charges in the self-doped Hubbard model is simply represented by unoccupied orbitals hybridizing purely local with the ones of the occupied sites.

The temperature behavior of the resistivity and the Hall coefficient is anomalous in  $\text{Yb}_4\text{As}_3$ . Both quantities show a non-monotonous temperature dependence and exhibit a maximum at a characteristic temperature. The characteristic temperatures differ for the two properties. Therefore, not only the maximum value of the resistivity and the Hall coefficient of the self-doped Hubbard model will be of interest but also the temperature dependence of the two properties. In this paper we calculate the density of states, resistivity and Hall coefficient of the self-doped Hubbard model in the vicinity of the metal-to-insulator transition using dynamical mean-field theory. In the next section we introduce the model and discuss the mapping of this multi-band model to an impurity model within the dynamical mean-field theory. The impurity model is studied numerically by an extension of the non-crossing approximation to a two-orbital impurity. We present the results in Sec. III, discuss the applicability of the self-doped Hubbard model to  $\text{Yb}_4\text{As}_3$  in Sec. IV and finally conclude in Sec. V.

## II. MODEL AND METHOD

The self-doped Hubbard model is given by

$$H = -(\Delta + \mu) \sum_{\vec{k}, \sigma} f_{\vec{k}\sigma}^\dagger f_{\vec{k}\sigma} + \sum_{\vec{k}, \sigma} \epsilon_{\vec{k}} f_{\vec{k}\sigma}^\dagger f_{\vec{k}\sigma} - \mu \sum_{\vec{k}, \sigma} c_{\vec{k}\sigma}^\dagger c_{\vec{k}\sigma} + V \sum_{\vec{k}, \sigma} \left( f_{\vec{k}\sigma}^\dagger c_{\vec{k}\sigma} + \text{h.c.} \right) + U \sum_i n_{i\uparrow}^f n_{i\downarrow}^f, \quad (1)$$

The model consists of a lattice of  $f$  orbitals described by the Hubbard Hamiltonian with on-site Coulomb repulsion  $U$ . Locally the  $f$  orbitals hybridize with additional orbitals called  $c$ . The hybridization strength is  $V$ . For an electron it is energetic favourable to occupy an  $f$  orbital. The energy difference between an occupied  $c$  orbital and an occupied  $f$  orbital is given by the charge-transfer energy  $\Delta$ . The filling is one electron per site, i.e., the system is quarter-filled. For  $V = 0$  the self-doped model reduces to a half-filled one-band Hubbard model. The Coulomb repulsion of the electrons is large,  $U > U_c$ , and the system is a Mott insulator. Here we have assumed a finite critical value of the Mott-Hubbard transition. For  $V \neq 0$  the mean occupation of  $f$  orbitals is smaller than one. We may say that for  $V = 0$  the electrons order in the sense that they only occupy the  $f$  subsystem. The charge ordered state is an insulator. A finite hybridization hinders the order to be perfect.

In Ref. 2 we have shown that for  $V = \infty$  the self-doped Hubbard model again reduces to a half-filled one. However, the effective Coulomb repulsion is reduced to  $U/4$  and the effective hopping to  $t/2$ . In a regime of  $U_c < U < 2U_c$  we therefore expect an insulator-to-metal transition to take place with increasing value of  $V$ . Unfortunately simple approximation schemes like slave-boson mean-field and alloy-analog approximation fail to reproduce this quantum transition. In this paper we apply the dynamical mean-field theory to the model.

Though we are aiming at the resistivity and the Hall coefficient of the model we first calculate the one-particle Green's function  $G(\vec{k}, \omega)$ . Given the noninteracting Green's function,  $G_0(\vec{k}, \omega)$ , of the self-doped Hubbard model

$$G_0^{-1}(\vec{k}, \omega) = \begin{pmatrix} \omega + \mu + \Delta - \epsilon_{\vec{k}} & -V \\ -V & \omega + \mu \end{pmatrix} \quad (2)$$

the self-energies are defined by Dyson's equation

$$G(\vec{k}, \omega) = \left( G_0^{-1}(\vec{k}, \omega) - \Sigma(\vec{k}, \omega) \right)^{-1}. \quad (3)$$

The dynamical mean-field theory assumes a momentum-independent self-energy  $\Sigma(\vec{k}, \omega) \rightarrow \Sigma(\omega)$ . In general the self-energy can be considered as a functional<sup>12</sup> of the full Green's function  $G(\vec{k}, \omega)$ . In particular the local approximated self-energy is only a functional of the local Green's function

$$G(\omega) = \frac{1}{N} \sum_{\vec{k}} G(\epsilon_{\vec{k}}, \omega). \quad (4)$$

The functional dependence is generated purely by the interaction term in the Hamiltonian. It is thus the same for an impurity model with the same interactions. Therefore, lattice and impurity model have the same self-energy provided we identify the Green's function  $\mathcal{G}(\omega)$  of the impurity model with  $G(\omega)$ . In the case of the self-doped Hubbard model the corresponding impurity model reads

---



---

(i)	$G_{ff}(\omega) = \sum_{nm}  P_1^\sigma(n, m) ^2 \langle\langle X_{nm}; X_{mn} \rangle\rangle_\omega$
(ii)	$\langle\langle X_{nm}; X_{mn} \rangle\rangle_\omega = \frac{1}{Z_{\text{Imp}}} \int_{-\infty}^{\infty} d\epsilon e^{-\beta\epsilon} \{p_n(\epsilon) P_m(\epsilon + \omega) - P_n^*(\epsilon - \omega) p_m(\epsilon)\}$
(iii)	$Z_{\text{Imp}} = \sum_m \int_{-\infty}^{\infty} d\epsilon e^{-\beta\epsilon} p_m(\epsilon)$
(iv)	$p_m(\epsilon) = -\frac{1}{\pi} \text{Im} P_m(\epsilon + i0^+), \quad P_m(z) = \int_{-\infty}^{\infty} d\epsilon \frac{p_m(\epsilon)}{z - \epsilon}$
(v)	$P_n(z) = \frac{1}{z - E_n - \Sigma_n^{(2)}(z)}$
(vi)	$\Sigma_n^{(2)}(z) = -\frac{1}{\pi} \sum_{m\sigma} \int_{-\infty}^{\infty} d\epsilon \text{Im} \mathcal{J}(\epsilon + i0^+) \{  P_1^\sigma(n, m) ^2 f(\epsilon) P_m(z + \epsilon) +  P_1^\sigma(m, n) ^2 f(-\epsilon) P_m(z - \epsilon) \}$

---



---

TABLE I. Summary of the used equations of the generalized NCA to solve approximatively the impurity problem

$$H_{\text{eff}} = H_{\text{cell}} + H_{\text{med}} \quad (5)$$

$$H_{\text{cell}} = -(\Delta + \mu) \sum_{\sigma} n_{\sigma}^f + U n_{\uparrow}^f n_{\downarrow}^f - \mu \sum_{\sigma} n_{\sigma}^c + V \sum_{\sigma} (f_{\sigma}^{\dagger} c_{\sigma} + \text{h.c.}) \quad (6)$$

$$H_{\text{med}} = \sum_{\vec{k}\sigma} E_{\vec{k}} d_{\vec{k}\sigma}^{\dagger} d_{\vec{k}\sigma} + \sum_{\vec{k}\sigma} \left( \Gamma_{\vec{k}} d_{\vec{k}\sigma}^{\dagger} f_{\sigma} + \text{h.c.} \right).$$

Note,  $H_{\text{eff}}$  just embeds a single unit-cell of the original lattice model in an effective medium. Following the discussions in Ref. 13 and 14 it is easy to show that the matrix equation

$$G(\omega) = \mathcal{G}(\omega) \quad (7)$$

can be fulfilled by choosing a single function

$$\mathcal{J}(\omega) = \sum_{\vec{k}} \frac{|\Gamma_{\vec{k}}|^2}{\omega - E_{\vec{k}}} \quad (8)$$

which describes the coupling of the  $f$  orbital to the bath. The integration in Eq. (4) can be performed analytically if we choose a semielliptic density of states

$$\rho_0(\epsilon) = \frac{1}{N} \sum_{\vec{k}} \delta(\epsilon - \epsilon_{\vec{k}}) = \frac{2}{\pi W^2} \sqrt{W^2 - \epsilon^2}. \quad (9)$$

The self-consistency (7) then reduces to

$$\mathcal{J}(\omega) = \frac{W^2}{4} G_{ff}(\omega). \quad (10)$$

In all our calculation we choose  $W = 1$  as unit of energy.

What remains is the calculation of the one-particle Green's function of the impurity problem (5). Here we make use of an extension of the non-crossing approximation<sup>16</sup> (NCA) to the case of more than two ionic propagators. Note, that the ‘‘impurity’’ in (5) has 16 eigenstates

$$H_{\text{cell}} = \sum_{m=1}^{16} E_m X_{mm} \quad (11)$$

and not only two as in the case of the  $U = \infty$  impurity Anderson model. In Eq. (11) we have introduced the Hubbard operators  $X_{nm} = |n\rangle\langle m|$ . The generalized NCA has been applied successfully to the finite- $U$  impurity Anderson model<sup>17</sup>, the Emery model in the dynamical mean-field theory<sup>15</sup>, and the Anderson-Hubbard<sup>13</sup> as well as the Kondo-Hubbard model<sup>14</sup> in this approximation. We just summarize the basic equations in Tab. I and refer the reader for further details to the literature, e.g. see Refs. 15,13,14. The coupled integral equations (v) and (vi) in Tab. I are solved numerically by introducing defect propagators<sup>18</sup> and making use of the fast Fourier transformation<sup>15</sup>. The  $f$  Green's function of the impurity model gives a new function  $\mathcal{J}(\omega)$  via Eq. (7) and the calculations are iterated until self-consistency is achieved.

We are now turning to the calculation of the resistivity and the Hall coefficient. In the self-doped Hubbard model the electrons can hop only from one  $f$  orbital on site  $i$  to an  $f$  orbital on a neighboring site  $i + \delta_{\alpha}$  ( $\alpha = x, y, z$  denotes the direction in space). The current operator of the model is therefore given by

$$j_{i+\frac{\delta_{\alpha}}{2}}^{\alpha} = \frac{i}{\hbar} a t \sum_{\sigma} (f_{i+\delta_{\alpha}\sigma}^{\dagger} f_{i\sigma} - f_{i\sigma}^{\dagger} f_{i+\delta_{\alpha}\sigma}), \quad (12)$$

where  $a$  is the lattice spacing. In momentum space the current operator reads

$$j_{\vec{q}}^{\alpha} = \frac{1}{\hbar} \sum_{\vec{p}\sigma} \left( \frac{\partial \epsilon_{\vec{p}}}{\partial p^{\alpha}} \right) f_{\vec{p}-\frac{\vec{q}}{2}\sigma}^{\dagger} f_{\vec{p}+\frac{\vec{q}}{2}\sigma}. \quad (13)$$

Given the current operator we can straightforwardly repeat the calculation of the conductivity in the case of the Hubbard model. It is not surprising that we end with the same expressions as in the case of the Hubbard model<sup>10</sup> just inserting the  $f$  spectral density

$$\sigma^{xx} = \frac{e^2 \pi}{6 \hbar a} \int_{-\infty}^{\infty} d\omega \left( -\frac{\partial f}{\partial \omega} \right) \int_{-1}^1 d\epsilon \rho_0(\epsilon) \rho_f^2(\epsilon, \omega) \quad (14)$$

$$\sigma_{\text{H}}^{xyz} = \frac{|e|^3 \pi^2 a}{27 \hbar^2 c} \int_{-\infty}^{\infty} d\omega \left( -\frac{\partial f}{\partial \omega} \right) \int_{-1}^1 d\epsilon \rho_0(\epsilon) \epsilon \rho_f^3(\epsilon, \omega). \quad (15)$$

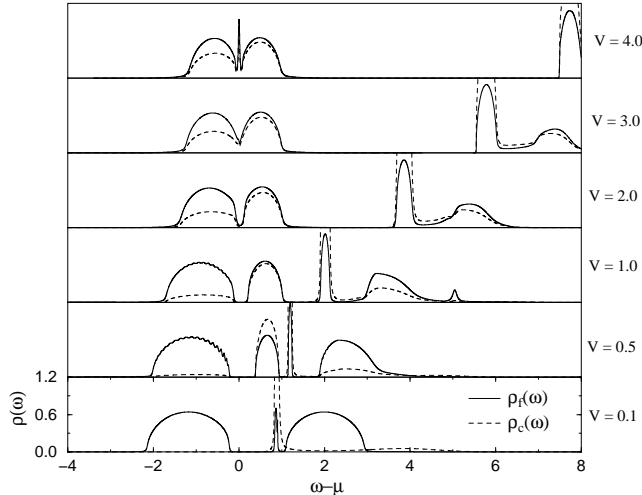


FIG. 1. Spectral density of the  $f$  and  $c$  orbitals in the self-doped Hubbard model for  $U = 3$ ,  $\Delta = 2$  and different values of the hybridization  $V$ . For  $V \geq 2.7$  the system is metallic and a sharp peak at the chemical potential is present

Here  $f(\omega) = [\exp(\beta\omega) + 1]^{-1}$  is the Fermi function. The derivation involves two steps. First, we consider the non-interacting case like in Ref. 19. Second, we mark that vertex corrections in the linear response diagrams vanish. Here the fact enters that the one-particle self-energy is momentum independent. In addition the special  $\vec{k}$ -dependence of the free propagators via  $\epsilon_{\vec{k}}$  and of the vertices via  $\frac{\partial \epsilon_{\vec{k}}}{\partial k^\alpha}$  (see Eq. (13)) is needed.<sup>10</sup> Because the vertex corrections vanish the free propagators in the expression for the noninteracting case can simply be replaced by full ones.

Given the conductivity  $\sigma^{xx}$  and the Hall conductivity  $\sigma_H^{xyz}$  we know the resistivity  $\rho_{xx} = 1/\sigma^{xx}$  and the Hall coefficient  $R_H = \sigma_H^{xyz}/(\sigma^{xx})^2$ . The units of the two transport properties are given by  $[\rho_{xx}] \approx [\hbar a/e^2] \approx 0.1 \text{ m}\Omega\text{cm}$  and  $[R_H] \approx [a^3/ec] \approx \frac{1}{c} 10^{-5} \text{ cm}^3/\text{C}$ , respectively. Note, the conductivities are given by the one-particle spectral function only

$$\rho_f(\epsilon, \omega) = -\frac{1}{\pi} \text{Im} G_{ff}(\epsilon, w + i0^+). \quad (16)$$

In particular, if  $\rho_f(\epsilon, \mu)$  vanishes for all energies  $\epsilon$ , i.e.,  $\rho_f(\mu) = 0$ , then also the conductivity vanishes for low temperatures. In this case the system is an insulator.

### III. RESULTS

When discussing the results we will frequently refer to experimental findings for the semimetal  $\text{Yb}_4\text{As}_3$ . In the next Section we will discuss the applicability of the self-doped Hubbard model to this rare-earth compound.

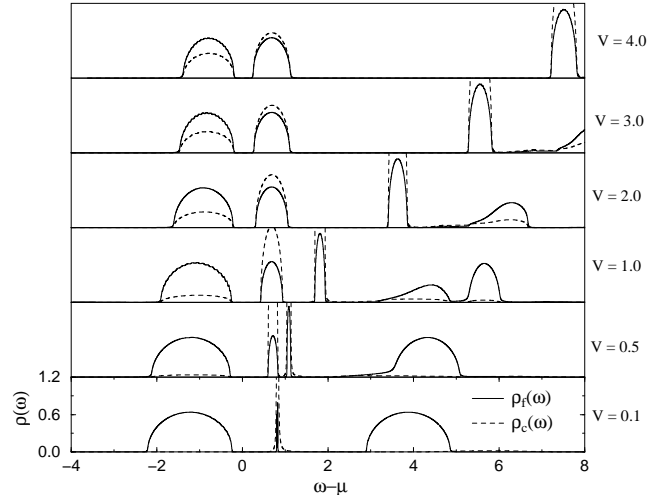


FIG. 2. Spectral density of the  $f$  and  $c$  orbitals in the self-doped Hubbard model for  $U = 5$ ,  $\Delta = 2$  and different values of the hybridization  $V$ . The system stays insulating independent of the value of  $V$ .

Heading for the metal-insulator diagram of the self-doped Hubbard model we first concentrate on the value of the  $f$  spectral function at the chemical potential  $\rho_f(\mu)$  for different values of the hybridization. In Fig. 1 we display the evolution of the spectral function of the model with increasing  $V$  and fixed values for  $U$  and  $\Delta$ . The  $f$  and  $c$  spectral functions are obtained by the treatment outlined in Sec. II. Within our approach the critical Coulomb repulsion of the Mott-Hubbard transition in the one-band Hubbard model is  $U_c = 1.77(5)$ . The chosen value of  $U = 3$  fullfills  $U_c < U < 2U_c$ . As expected for this value of  $U$  the model undergoes an insulator-to-metal transition. For  $V < 3$  we obtain  $\rho_f(\mu) = 0$  and the system is an insulator. For  $V \geq 3$  we find a finite value  $\rho_f(\mu) \neq 0$  and the model is a metal. Increasing the resolution in  $V$  we obtain the value  $V_c \approx 2.7$  for the critical hybridization of the transition. Next, we consider the case of a very large Coulomb repulsion  $U = 5$ , i.e.,  $U > 2U_c$ . In Fig. 2 we demonstrate that the gap between the filled band and the lowest empty band never closes. The density of states at the chemical potential vanishes for all values of the hybridization. This shows clearly that the insulator-to-metal transition is restricted to a parameter region  $U_c < U < 2U_c$ . In Fig. 3 we display the resulting metal-insulator diagram of the self-doped Hubbard model in the  $(U, V)$ -plane for two different values of the charge transfer energy.

Qualitatively a phase diagram of this form was already predicted in Ref. 2. Indeed, the bands in the spectral function of the lattice model evolve like the transition energies of the single two-orbital impurity ( $H_{\text{cell}}$  in Eq. (5)). Therefore no sophisticated calculations are required to determine roughly the position of the cen-

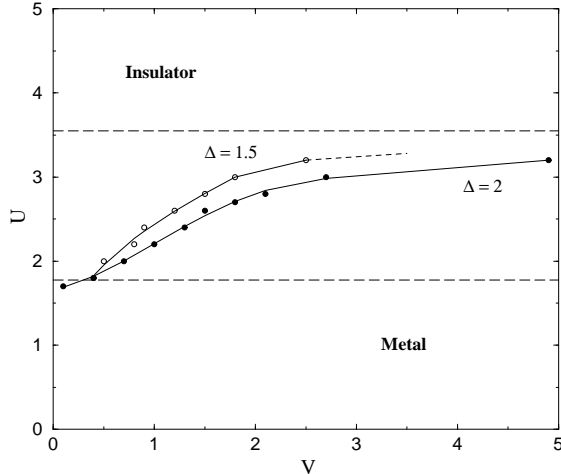


FIG. 3. Metal-insulator diagram of the self-doped Hubbard model for  $\Delta = 2$  (full circles) and  $\Delta = 1.5$  (open circles). The lines are guide to the eye and separate the metallic from the insulating regime. Transitions between the two states are limited to a region between  $U_c = 1.775$  and  $2U_c = 3.55$  marked by horizontal dashed lines.

ters of bands. We denote the possible transitions of the single two-orbital impurity by  $(f^1 c^0) \rightarrow (f^n c^m)$ . The correspondence of the respective transition energies and the band energies allows us to classify the occupied band below the chemical potential as  $(f^0 c^0)$ -band and the unoccupied bands above  $\mu$  as  $(f^1 c^1)_{s-}$ ,  $(f^1 c^1)_{t-}$  and  $(f^2 c^0)$ -bands (here s and t refers to singlet and triplet). Lattice effects show up in the ratio between  $f$  and  $c$  weight constituting a single band. For example, the occupation number of  $c$  orbitals is larger in the lattice model than in the two-orbital impurity marking a larger  $c$  weight in the occupied  $(f^0 c^0)$ -band. This is a simple consequence of quantum fluctuations between different impurity configurations in the ground state of the lattice model.

Nevertheless, the most prominent feature of the lattice model is the appearance of a sharp Kondo-like resonance close to the chemical potential. The temperature dependence of the resonance is shown in Fig. 4. The peak arises below a characteristic temperature  $T_0$ . Regarding the hybridization dependence of the resonance we state that it becomes narrower and shows up at a lower temperature  $T_0(V)$  when we approach the insulating state from the metallic side, i.e., when we regard the limit  $V \rightarrow V_c^+$ . Note, that for temperatures just above  $T_0$   $\rho_f(\mu)$  is a monotonously decreasing function in this limit. Therefore the observed behavior of  $T_0$  is very similar to the well-known dependence of the Kondo temperature on the density of states  $T_K \sim \exp(-b/\rho(\mu))$ . The usual Kondo effect can be interpreted in terms of the resonant-level model.<sup>20</sup> The conduction electrons with energies close to  $\mu$  are virtually bound to localized electrons due to resonance scattering. In a similar way one may assign the

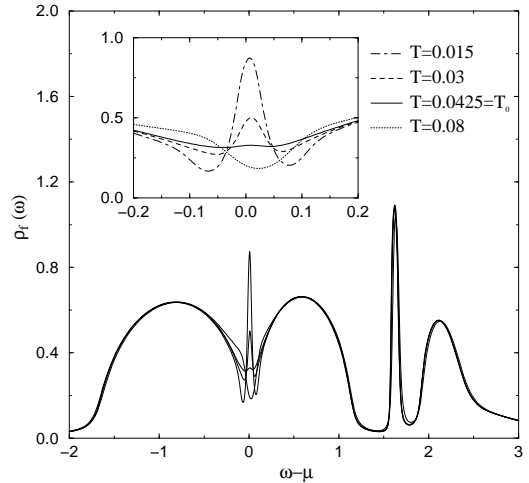


FIG. 4. Temperature dependence of the  $f$  spectral density of the self-doped Hubbard model with parameters  $(U, \Delta, V) = (1.8, 2, 0.6)$ . The inset shows the enlarged frequency region close to the chemical potential. Below the temperature  $T_0$  a sharp peak arises at the chemical potential.

resonance seen in our calculations to a band-Kondo effect where the conduction electrons are virtually bound not to localized but to moving electrons. This “band-Kondo effect” is a typical feature of strongly correlated metals treated within the dynamical mean-field theory. It occurs also in the one-band Hubbard model. It is still a matter of dispute if the effect is physical or a shortcoming of the mapping of the lattice model to an impurity model as done within the dynamical mean-field theory. But at least in the case of the Hubbard model there are indications that the effect can be seen also by other methods.<sup>21,22</sup>

The strong temperature dependence of the spectral density close to the chemical potential causes a strong temperature dependence of the resistivity. In Fig. 5 we show this dependence as obtained by the treatment outlined in Sec. II. First we focus on the magnitude of the resistivity. The resistivity increases when we decrease the hybridization, i.e., when we approach the insulating regime. In fact we expect a diverging resistivity in the limit  $V \rightarrow V_c^+$  because the conductivity vanishes in an insulator. This is the key idea. In the vicinity of a quantum transition to an insulator we can obtain large values for the resistivity and the Hall coefficient implying semimetallic behavior. In Fig. 5 the order of magnitude of the resistivity is  $1\text{m}\Omega\text{cm}$ , i.e., the same as observed in  $\text{Yb}_4\text{As}_3$ . Note, that large values of  $\rho$  and  $R_H$  do not imply that the occupation number of the  $c$  orbitals  $n^c = 1 - n^f$  have to be small. Large values are possible for every  $n_c$  in striking contrast to a simple Drude picture when assuming the charge carriers in the system are given by the missing electrons in the  $f$  subsystem. We stress this

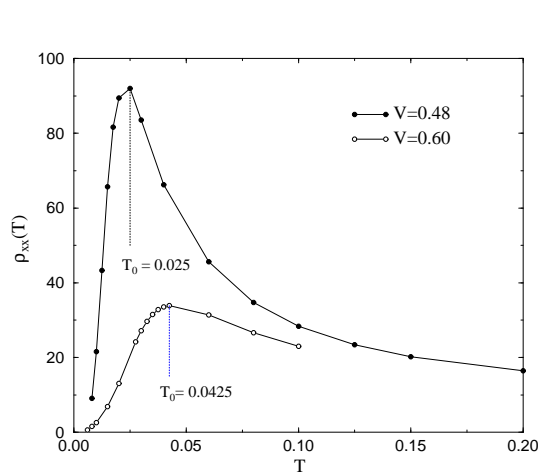


FIG. 5. Temperature dependence of the specific resistivity in the self-doped Hubbard model. The unit of the the resistivity is  $0.1\text{m}\Omega\text{cm}$ . Magnitude and position of the maximum shift with the value of the hybridization  $V$ .

point because in  $\text{Yb}_4\text{As}_3$  there is experimental evidence<sup>7</sup> that the number of missing holes in the  $\langle 111 \rangle$ -chains is not identical with the low carrier concentration obtained from the large Hall coefficient.

As function of temperature the resistivity shows a maximum at a characteristic temperature  $T_0$ . This temperature is identical with the one discussed above, i.e., the temperature where the sharp resonance arises in the spectral function. As seen in Fig. 5 and as discussed before  $T_0$  is larger for parameter values deeper in the metallic regime of the self-doped Hubbard system.  $\text{Yb}_4\text{As}_3$  can be tuned to a more insulating or metallic state (indicated by the value of the resistivity) by applying pressure<sup>23</sup> or substituting P or Sb for As.<sup>24,25</sup> Indeed, the experimentally observed characteristic temperature shows the expected behavior. In samples with a lower (more metallic) resistivity  $T_0$  becomes larger as compared to samples with a higher resistivity. Note, that the resonance appears also in the  $c$  spectral function (see Fig. 1 or Fig. 7). Concerning  $\text{Yb}_4\text{As}_3$  we may interpret the  $c$  orbitals as As  $p$  band with zero bandwidth. However, in  $\text{Yb}_4\text{As}_3$  the  $p$  band is broad and especially the holes in this band should contribute to transport<sup>26</sup>. We may conjecture that also the  $p$  holes reveal the described low temperature scale  $T_0$  (see also the discussion in the next Section). This is known for the case of a periodic Anderson model where also a non-monotonous temperature dependence of the resistivity is obtained.<sup>27</sup>

The enhanced  $f$  spectral function close to the chemical potential indicates heavy masses of the charge carriers at low temperatures. Unfortunately, our approach does not allow us to perform the limit  $T \rightarrow 0$ . It is well-known<sup>28</sup> that the non-crossing approximation underestimates the

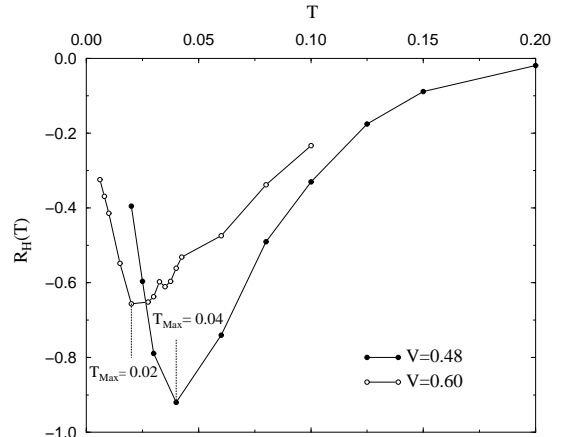


FIG. 6. Temperature dependence of the Hall coefficient in the self-doped Hubbard model. The unit of the Hall coefficient is  $\frac{1}{c}10^{-5}\text{cm}^3/\text{C}$ . Magnitude and position of the minimum shift with the value of the hybridization  $V$ .

absolute value of the imaginary part of the self-energy of the single-impurity Anderson model. This failure will be enhanced in the self-consistent adjustment of the hosting bath of conduction electrons leading to an unphysical change of sign of the self-energy at low temperatures.<sup>29</sup> Therefore we cannot proof the relation  $\rho(T) = AT^2$  and we cannot calculate the coefficient  $A$ . However, note that in Fig. 5 the onset of a  $T^2$ -behavior can be seen at least for the case of  $V = 0.6$ .

We now turn to the temperature dependence of the Hall coefficient as displayed in Fig. 6. For discussion we want to compare qualitatively the calculated Hall coefficient with the one measured in  $\text{Yb}_4\text{As}_3$ . First of all the Hall coefficient of the self-doped Hubbard model is negative whereas it is positive in  $\text{Yb}_4\text{As}_3$ . From our point of view this has to be expected. In the model electrons order in the sense that they prefer to occupy the  $f$  sub-system. In  $\text{Yb}_4\text{As}_3$  however holes in the  $4f$ -shells of the Yb-ions are predominantly confined to the  $\langle 111 \rangle$ -chains. So there is a different sign for the charge carriers which should show up in the Hall coefficient (see also the modified model in the next Section). Second, the magnitude of the Hall coefficient seems to be wrong. In Fig. 6 it is still five orders of magnitude too small. This rather small value of the Hall coefficient is caused by the still very symmetric spectral function close to the chemical potential (see Fig. 4). In this respect the chosen values of the hybridization (about 25% of the unperturbed  $f$  bandwidth  $2W$ ) are too large. Nevertheless, as we have stressed before the value of the Hall coefficient can be tuned by choosing parameter values of the model closer to the metal-to-insulator transition. Close to the transition arbitrary large values for the Hall coefficient may be

obtained.

Keeping this in mind we find indeed an anomalous temperature dependence of the Hall coefficient as in experiment with a characteristic temperature  $T_{\text{Max}}$ . In the case of  $V = 0.6$  in Fig. 6 this characteristic temperature is smaller than the one found in the resistivity (see Fig. 5). The relation  $T_0/T_{\text{Max}} \approx 2.13$  is close to the experimental one  $T_0/T_{\text{Max}} \approx 1.75$ . As we will point out in the next Section, the self-doped Hubbard model is not a model simplifying the band structure of  $\text{Yb}_4\text{As}_3$  close to the chemical potential. Therefore, we only want to discuss possible implications of the Coulomb interaction of the charge carriers on the transport properties. If we would e.g. identify the temperature  $T_0 = 0.0425$  with the experimental one of 140K we obtain for the  $f$  bandwidth  $2W \approx 0.6\text{eV}$ . The LSDA+ $U$  approach which will be reviewed in the next Section gives a value of  $2W = 0.007\text{eV}$ . But even qualitatively there is still an essential difference. Surprisingly  $T_{\text{Max}}$  decreases with increasing value of the hybridization. This behavior of  $T_{\text{Max}}$  is just opposite to the one of  $T_0$ . In experiment both  $T_0$  and  $T_{\text{Max}}$  behave the same. Especially the ratio  $\rho(T)/R_{\text{H}}(T)$ , i.e., the inverse Hall mobility of the charge carriers, is independent of the applied pressure. It is not clear if our finding for the behavior of  $T_{\text{Max}}$  in the model depends on the parameter regime and possibly change closer to the metal-to-insulator transition or not.

#### IV. THE SEMIMETAL $\text{Yb}_4\text{As}_3$

In the preceding Section we have presented the semimetal  $\text{Yb}_4\text{As}_3$  as possible candidate for a compound which can be described by the self-doped Hubbard model. In this Section we will describe the properties of this compound in more detail. We want to argue that it is indeed justified to compare the transport properties of the self-doped Hubbard model and of  $\text{Yb}_4\text{As}_3$  as we have already done.

$\text{Yb}_4\text{As}_3$  is an example of a low-carrier heavy-fermion system<sup>9</sup>. Below 100K a linear specific heat is found with a large coefficient  $\gamma \approx 200 \text{ mJ}/(\text{molK}^2)$ . The Sommerfeld-Wilson ratio is of order unity. The large Hall coefficient at low temperatures indicates an extremely small concentration of  $\delta = 0.3 \times 10^{-3}$  positive charge carriers/Yb-atom. The large Hall coefficient and the large residual resistivity of  $1 \text{ m}\Omega\text{cm}$  at low temperatures classify  $\text{Yb}_4\text{As}_3$  as a semimetal. In  $\text{Yb}_4\text{As}_3$ , all Yb-atoms are aligned on four families of chains. Assuming trivalent As the ratio of Yb-ions is  $\text{Yb}^{3+} : \text{Yb}^{2+} = 1 : 3$ . A  $\text{Yb}^{3+}$ -ion has one hole in the  $f$  shell ( $4f^{13}$ ) and shows a magnetic moment due to Hund's rule coupling. In a sequence of papers<sup>3-6</sup> Schmidt, Thalmeier and Fulde suggests that at low temperatures the  $\text{Yb}^{3+}$ -ions are confined to one of the four chain systems, e.g., parallel  $\langle 111 \rangle$ -chains. The low energy excitations of these quasi-one-dimensional spin chains explain the specific heat including the large  $\gamma$ -coefficient.

However, due to the strong Coulomb repulsion of the holes and the large distance of the  $\text{Yb}^{3+}$ -sites within one chain a perfect ordered state would imply an insulator. Because  $\text{Yb}_4\text{As}_3$  is a semimetal a small fraction of holes have to be redistributed either on the As-atoms or on the other three chain systems, i.e., the  $\langle 111 \rangle$ -chains have to be "self-doped". It is tempting to identify this small fraction of holes with the low concentration of charge carriers seen in the Hall coefficient. The charge ordering of the  $\text{Yb}^{3+}$ -ions is meanwhile experimentally confirmed.<sup>7,8</sup> However, the number of missing holes in the  $\langle 111 \rangle$ -chains cannot be exactly measured. Note, that the polarized neutron diffraction experiment suggest that this number is not small but of the order of several percent.

During the completion of our work, the electronic structure of  $\text{Yb}_4\text{As}_3$  has been investigated using energy band calculations within the so-called LSDA+ $U$  approach<sup>26</sup>. The calculations take into account the possibility of hole occupation on the Yb-sites of the  $\langle 111 \rangle$ -chains and on the As-sites but not on the remaining three chains system. In result a very narrow  $\text{Yb}^{3+} 4f$  hole band is obtained close to the top of a broad As  $p$  band. The Fermi energy is pinned to the bottom of the  $4f$  hole band. From this band structure indeed a very small occupation number of holes on the As-sites results comparable to the small carrier number estimated from the Hall coefficient. This finding is independent from the chosen value of  $U$  over a wide range of several eV. One should mention that the possible hole distributions in the used approach are too restrictive to deal with valence fluctuating systems like  $\text{Yb}_4\text{Bi}_3$  and  $\text{Yb}_4\text{Sb}_3$  which do not show a charge ordering transition. Only the  $p$  holes should contribute to transport properties because there is no direct  $ff$ -hopping. This explain correctly the sign and magnitude of the Hall coefficient.

Some questions remain intriguing. In agreement with Fermi-liquid behavior the resistivity is found to be of the form  $\rho(T) = \rho_0 + AT^2$  with a large coefficient  $A \approx 0.84 \mu\Omega\text{cm}/\text{K}^2$ . It is hard to understand which scattering mechanism of the  $p$  holes can lead to such high effective masses in transport. Not understood at all is the temperature dependence of the resistivity and the Hall coefficient of  $\text{Yb}_4\text{As}_3$ . Both quantities show a non-monotonous temperature dependence and exhibit a maximum at a characteristic temperature. The characteristic temperatures differ for the two properties.

Two comments seem to be appropriate. First of all, the band-structure results question strongly the validity of the self-doped Hubbard model for the compound under consideration  $\text{Yb}_4\text{As}_3$ . In this compound the transport seems to be purely due to the few charge carriers in the nearly empty charge reservoir, e.g., the holes on the As-sites. In the self-doped Hubbard model however the electrons in the  $c$ -states do not contribute to the transport properties of the model at all. Moreover, the perfect charge ordered state, e.g., all holes confined to the  $\langle 111 \rangle$ -chains, is a Mott insulator of a very extreme type because the kinetic energy of the holes on the Yb-sites

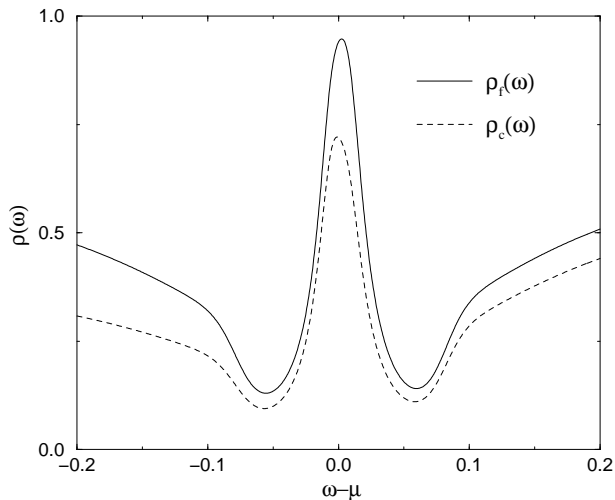


FIG. 7. Spectral density of the  $f$  and  $c$  orbitals in the self-doped Hubbard model for  $U = 3$ ,  $\Delta = 2$  and  $V = 4$ . In comparison with Fig. 1 the enlarged frequency region close to the chemical potential is shown.

is nearly zero. Therefore, a suitable model Hamiltonian is still of the form of Eq. (1) but with two important changes. The filling should be three electrons per site and the Coulomb repulsion should be suffered by the  $c$ -electrons. In this modified version the  $f$ -subsystem (and not  $c$ ) represents the As sites with nearly no holes and the  $c$ -subsystem represents the  $\text{Yb}^{3+}$ -ions occupied by nearly one hole per site. In a future work we will investigate this model. Nevertheless, we believe that the modified model behaves quite similar to the self-doped Hubbard model. Following the arguments outlined in Ref. 2 an insulator-to-metal transition as function of the hybridization have to be expected for both, the self-doped Hubbard model and the modified model. In Fig. 7 we show the  $f$  and  $c$  spectral functions of the self-doped Hubbard model in the metallic regime. A sharp peak close to the chemical potential is seen in both, the  $f$  and the  $c$  spectral function. The interaction induced many-body effects of the correlated subsystem are carried over to the system of the uncorrelated orbitals. Therefore, the similarity of the self-doped Hubbard model with the proper model of  $\text{Yb}_4\text{As}_3$  holds despite the fact that the conductivity of the modified model is given by the spectral function of the uncorrelated orbitals. In conclusion, it is justified to compare here some findings for the self-doped Hubbard model with transport measurements of  $\text{Yb}_4\text{As}_3$ .

We can argue in a slightly different way. In the charge ordered phase of  $\text{Yb}_4\text{As}_3$  the Coulomb repulsion constrains the holes in the  $4f$ -shell of the Yb-ions to be localised. The long range part of the repulsion restricts the holes to chains in  $\langle 111 \rangle$ -direction. The on-site part hinders the holes to move along a single chain. This implies that the  $4f$ -spectral density is split into bands separated by gaps which we may call charge order and Mott-

Hubbard gaps, respectively. The charge order gap will be of the order of the transition temperature  $T_c \approx 295\text{K}$  and is much smaller than the Mott-Hubbard gap of several eV. Therefore, the relevant gap for electron excitations is the charge order gap and not the Mott-Hubbard gap. However, the charge order gap in the  $4f$ -spectral density is a true many-particle effect and cannot be explained by the change of the unit cell between the charge disordered and the charge ordered phase. Note, the size of the unit cell is unchanged in the charge order transition. The cell is only distorted, changing from cubic to trigonal. The distortion of the unit cell has only little influence on the electronic structure of  $\text{Yb}_4\text{As}_3$ , as shown in Ref. 26. We believe that the charge order gap resembles much more a Mott-Hubbard gap than it resembles a gap in an usual band insulator. The physics of the charge ordering is not included in the self-doped Hubbard model. But what is considered in the used model is the effect of hybridization between a correlated (Hubbard like) band and an uncorrelated band.

The second comment concerns the temperature dependence of the resistivity and the Hall coefficient of  $\text{Yb}_4\text{As}_3$ . On the first sight it resembles the one found in other heavy-fermion compounds like  $\text{UPt}_3$ . In  $\text{UPt}_3$  the anomalous Hall conductivity arises from skew-scattering of the charge carriers<sup>30</sup>. As a consequence, the anomalous Hall coefficient should be proportional to the square of the resistivity for temperatures smaller than  $T_{\text{Max}}$ , the temperature for which a maximum in the Hall coefficient is observed. However, in  $\text{Yb}_4\text{As}_3$  the relation  $R_H \sim \rho^2$  is not fulfilled in the temperature regime from 80K down to 4K. Moreover, the zero-temperature value of the Hall coefficient in  $\text{Yb}_4\text{As}_3$  is at least three orders of magnitude larger than in other heavy-fermion compounds with a positive Hall coefficient. We therefore exclude skew-scattering as possible mechanism to explain the experimental data.

## V. CONCLUSION

In conclusion, we extended the Hubbard model by coupling one additional orbital per site via hybridization to the Hubbard orbitals. The Coulomb repulsion is supposed to be large,  $U > U_c$ , where  $U_c$  denotes the critical Coulomb repulsion for the Mott-Hubbard transition in the one-band Hubbard model. We calculated the spectral function, resistivity and Hall coefficient of the “self-doped” Hubbard model using dynamical mean-field theory. To this end the lattice model is mapped onto an impurity model in which a unit cell of the lattice is embedded self-consistently in a bath of free electrons. The impurity model is studied numerically by an extension of the non-crossing approximation to a two-orbital impurity.

The self-doped Hubbard model is an insulator only in a restricted parameter regime. The hybridization with

the added orbitals drives an insulator-to-metal transition, provided the Coulomb repulsion fulfills the constraint  $U_c < U < 2U_c$ . This is a correlation driven metal-insulator transition in a non particle-hole symmetric case. In the vicinity of the transition to an insulator the resistivity and the Hall coefficient become very large. Therefore the model serves as a model for semimetallic behavior in systems where the Coulomb interactions of the charge carriers nearly block their movement. The number of missing electrons in the Hubbard subsystem, i.e., the occupation number of the additional orbitals, can not be interpreted as number of charge carriers seen in the transport properties. A simple Drude analysis fails for this type of mechanism leading to semimetallic behavior.

In the semimetallic regime the resistivity and the Hall coefficient show an unusual temperature dependence. Both,  $\rho(T)$  and  $|R_H(T)|$ , exhibit a maximum at a characteristic temperature. The characteristic temperatures for the resistivity  $T_0$  differs from the one of the Hall coefficient  $T_{\text{Max}}$ . Depending on the parameter regime either  $T_0 < T_{\text{Max}}$  or  $T_0 > T_{\text{Max}}$  is possible. The characteristic temperatures change considerably when varying the hybridization and tuning the system into a more insulating or metallic state. At  $T_0$  a resonance arises in the spectral function close to the chemical potential. This resonance can be assigned to a Kondo-like effect for band electrons. The enhanced spectral weight at the chemical potential indicates heavy masses for the charge carriers.

We compared our findings with measurements of the resistivity and the Hall coefficient for the semimetal  $\text{Yb}_4\text{As}_3$  including pressure and substitution experiments. Although the self-doped Hubbard model is not a simplified model extracted from band structure calculations we found surprising similarities. We take this as indication that the anomalous transport properties of  $\text{Yb}_4\text{As}_3$  can be indeed assigned to the Coulomb interaction of the charge carriers which is not treated adequate in standard band structure calculations. This should be true even when the transport properties are dominated by As  $p$  holes. At least in the model the interaction induced many-body effects of the Hubbard subsystem are carried over to the system of the additional orbitals. Nevertheless, to obtain final conclusive results the band structure of  $\text{Yb}_4\text{As}_3$  have to be used as input for a simple model which still can be treated within the dynamical mean-field theory. This is left for future work.

#### ACKNOWLEDGMENTS

We would like to thank P. Fulde, B. Schmidt and P. Thalmeier for useful discussions and J. Schmalian for numerical advice.

- <sup>1</sup> N.F. Mott, Proc. phys. Soc. A **62**, 416 (1949)
- <sup>2</sup> S. Blawid, H.A. Tuan, T. Yanagisawa and P. Fulde, Phys. Rev. B **54**, 7771 (1996)
- <sup>3</sup> P. Fulde, B. Schmidt and P. Thalmeier, Europhys. Lett. **31**, 5 (1995)
- <sup>4</sup> B. Schmidt, P. Thalmeier and P. Fulde, Physica B **223-224**, 373 (1996)
- <sup>5</sup> B. Schmidt, P. Thalmeier and P. Fulde, Europhys. Lett. **35**, 109 (1996)
- <sup>6</sup> B. Schmidt, P. Thalmeier and P. Fulde, Physica B **237-238**, 221 (1997)
- <sup>7</sup> M. Kohgi, K. Iwasa, A. Ochiai, T. Suzuki, J.-M. Mignot, B. Gillon, A. Gukasov, J. Schweizer, K. Kakurai, M. Nishi, A. Dönni and T. Osakabe, Physica B **230-232**, 638 (1997)
- <sup>8</sup> M. Rams, K. Kólas, K. Tomala, A. Ochiai and T. Suzuki, Hyperfine Interactions **97-98**, 125 (1996)
- <sup>9</sup> A. Ochiai, T. Suzuki and T. Kasuya, J. Phys. Soc. Jpn. **59**, 4129 (1990)
- <sup>10</sup> T. Pruschke, M. Jarell and J.K. Freericks, Adv. Phys. **44**, 187 (1995)
- <sup>11</sup> A. Georges, G. Kotliar, W. Krauth and M. Rozenberg, Rev. Mod. Phys. **68**, 13 (1996).
- <sup>12</sup> G. Baym, Phys. Rev. **127**, 1391 (1962)
- <sup>13</sup> T. Schork and S. Blawid, Phys. Rev. B **56**, 6559 (1997).
- <sup>14</sup> T. Schork and S. Blawid, submitted to Phys. Rev. B
- <sup>15</sup> P. Lombardo, M. Avignon, J. Schmalian and K.-H. Bennemann, Phys. Rev. B **54**, 5317 (1996).
- <sup>16</sup> N.E. Bickers, Rev. Mod. Phys. **59**, 845 (1987)
- <sup>17</sup> T. Pruschke and N. Grewe, Z. Phys. B **74**, 439 (1989)
- <sup>18</sup> N.E. Bickers, D.L. Cox and J.K. Wilkins, Phys. Rev. B **36**, 2036 (1987)
- <sup>19</sup> P. Voruganti, A. Golubentsev and S. John, Phys Rev. B **45** 13945 (1992)
- <sup>20</sup> A.C. Hewson, *The Kondo Problem to Heavy Fermions* (Cambridge University Press, Cambridge, 1993)
- <sup>21</sup> N. Bulut, D.J. Scalapino and S.R. White, Phys. Rev. Lett. **72** 705 (1994)
- <sup>22</sup> R. Preuss, W. Hanke and W. von der Linden, Phys. Rev. Lett. **75** 1344 (1995)
- <sup>23</sup> Y. Okunuki, N. Môri, A. Ochiai, Y. Haga and T. Suzuki, J. Phys. Soc. Jpn. **64** 533 (1995)
- <sup>24</sup> A. Ochiai, H. Aoki, T. Suzuki, R. Helfrich and F. Steglich, Physica B **230-232** 708 (1997)
- <sup>25</sup> H. Aoki, A. Ochiai, T. Suzuki, R. Helfrich and F. Steglich, Physica B **230-232** 698 (1997)
- <sup>26</sup> V.N. Antonov, A.N. Yaresko, A.Ya., Perlov, P. Thalmeier, P. Fulde, P.M. Oppeneer and H. Eschrig, submitted to Phys. Rev. B
- <sup>27</sup> G. Czyczoll, Q. Qin and H. Schweitzer, Physica B **186-188** 844 (1993)
- <sup>28</sup> D.L. Cox and N. Grewe, Z. Phys. B **71** 321 (1988)
- <sup>29</sup> T. Pruschke, D.L. Cox and M. Jarell, Phys. Rev. B **47** 3553 (1993)
- <sup>30</sup> H. Kontani and K. Yamada, J. Phys. Soc. Jpn. **63** 2627 (1994)